Hollow Nanostructures

DOI: 10.1002/ange.200602403

Synthesis of Platinum Nanocages by Using Liposomes Containing Photocatalyst Molecules**

*Yujiang Song, Robert M. Garcia, Rachel M. Dorin, Haorong Wang, Yan Qiu, and John A. Shelnutt**

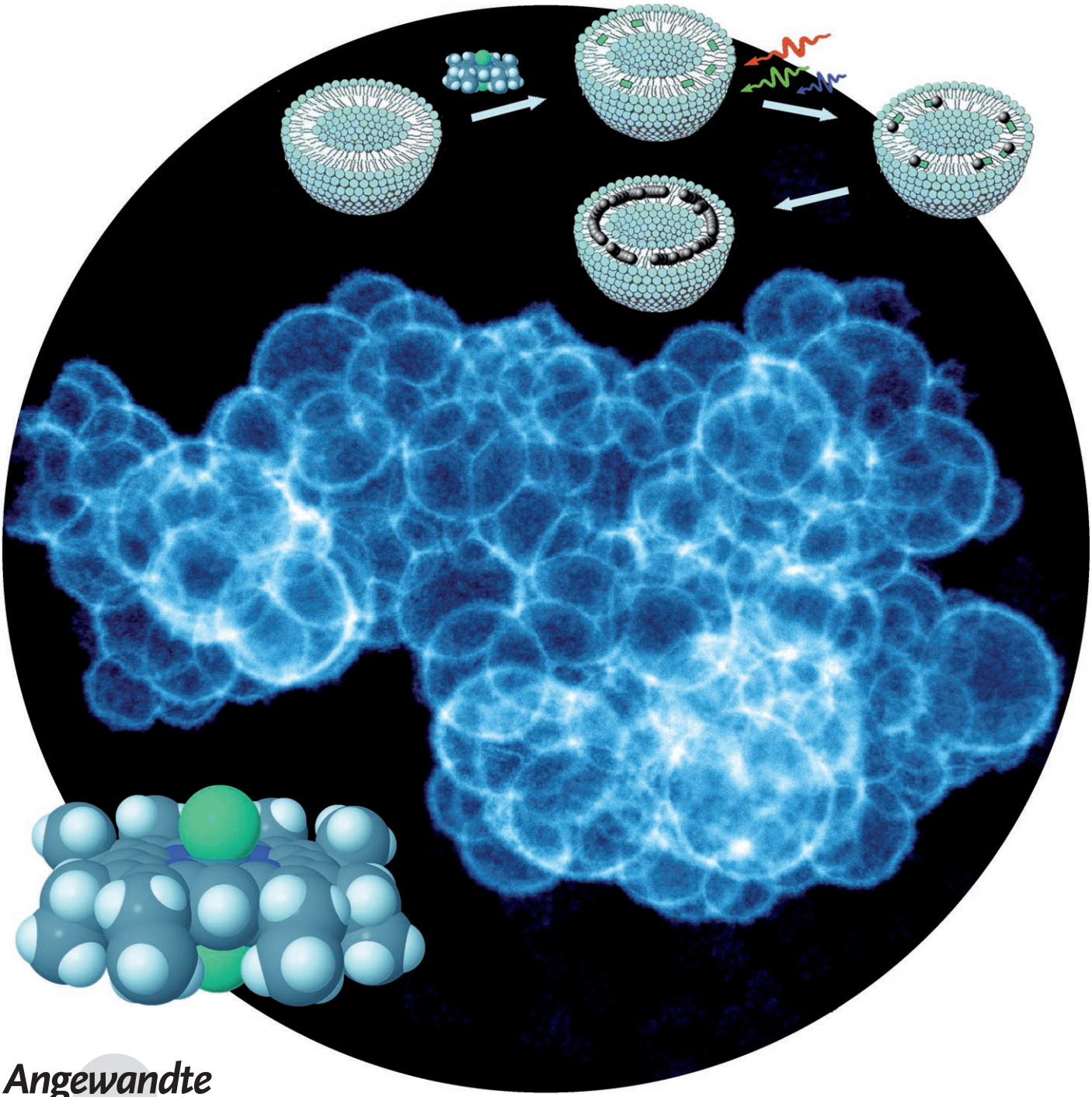

Hollow nanospheres are of interest because of their tunable structural features, including shell thickness, interior cavity size, and chemical compositions. In particular, metallic hollow nanospheres have drawn much attention because of their high surface area, low density, material economy, cost reduction, and in some cases surface permeability compared with solid nanospheres. These unique properties lead to a diverse range of reported biomedical,[1,2] catalytic,[3] and optical[4] applications.

The synthesis of metallic hollow nanospheres is limited mainly to two approaches. One is the deposition of metal onto solid nanospheres of silica,[5–7] latex,[8,9] metal,[4,10–13] and other materials,[14–16] with subsequent removal of the templating core, typically by replacement reactions[10–13,17] or corrosion.[4,18,19] The other approach is the co-assembly[20–22] of metallic nanoparticles with organic molecules into hollow nanospheres. A disadvantage of these approaches is that the hollow nanospheres are mainly composed of discrete nanoparticles, making them relatively unstable and apparently precluding the possibility of making hollow nanospheres larger than 100 nm in diameter with thin 2–3-nm shells.

Herein, we report a new method for making hollow metallic nanospheres using templating liposomes containing photocatalyst molecules. Platinum is used to demonstrate this concept in light of its catalytic activity in many applications.[23,24] This synthetic approach gives novel porous platinum nanocages with 2-nm shell thickness and diameters up to 200 nm. These cages are assembled from joined dendritic nanosheets instead of individual nanoparticles. Synthetic control over their structure was achieved by simply varying the concentration of platinum complex. The dendritic character of the constituent nanosheets makes the hollow spheres highly porous.

Scheme 1 shows the proposed synthesis method that leads to the hollow platinum nanocages. The unilamellar liposomes containing hydrophobic Sn^{IV} octaethylporphyrin (SnOEP) in the liposomal bilayer (Scheme 1B) were prepared by a process of solvent evaporation, hydration, and extrusion.[25] The UV/Vis spectrum of SnOEP in the liposomal bilayer (see Supporting Information Figure S1) shows that the porphyrin molecules are monodisperse. Photocatalytic reduction of Pt complex produces metal seed particles upon irradiation of the liposomes containing the SnOEP with white light; the Pt nanoparticles, which are seeds for the dendritic Pt nanosheets, are rapidly generated according to the simplified Equations (1)–(3) where ascorbic acid (AA) is used as the electron donor (ED) and Pt^{2+} is from aged aqueous platinum salt (K_2PtCl_4).

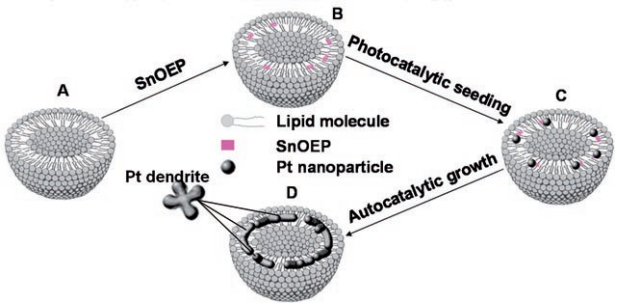

Scheme 1. Diagram of steps in the synthesis of spherical platinum nanocages. A) cross-section view of a liposome (cholesterol molecules are left out for simplicity); B) a liposome containing SnOEP molecules within its bilayer; C) a liposome with Pt seed particles grown photocatalytically in the vicinity of SnOEP molecules; D) a liposome with joined Pt dendritic nanosheets after autocatalytic growth of the original seeds.

$$\mathrm{SnOEP} + h\nu \rightarrow \mathrm{SnOEP}^* \quad (1)$$

$$\mathrm{SnOEP}^* + \mathrm{ED} \rightarrow [\mathrm{SnOEP}]^{-\cdot} + \mathrm{ED}_{ox} \quad (2)$$

$$2\,[\mathrm{SnOEP}]^{-\cdot} + \mathrm{Pt}^{2+} \rightarrow 2\,\mathrm{SnOEP} + \mathrm{Pt}^0 \quad (3)$$

AA and a prevalent hydrolyzed form of the Pt salt ($Pt(H_2O)_2Cl_2$) are both uncharged at pH 3, and thus electron transport between the SnOEP inside the bilayer and these compounds is likely. Presumably the Pt seed particles grow in the vicinity of SnOEP molecules as indicated in Scheme 1C; we have previously presented evidence that the Pt seeds reside within the liposomal bilayer.[25] When the seed particles reach a certain size they become catalytic and begin to grow by catalytic oxidation of ascorbic acid and reduction of Pt complex at their surfaces,[25–27] forming dendritic nanosheets as indicated in Scheme 1D (also see Figure 1c,d). The dendritic growth continues until the Pt complex is exhausted, thus the size of the Pt dendrites is determined by the total Pt complex available and the number of seeds produced.

The key to making the nanocages is to incorporate a large number of SnOEP molecules into each liposome to ensure that the neighboring nascent seed particles are close enough for the dendrites to grow together when the appropriate amount of platinum complex is provided. In this way, many small circular dendritic sheets grow until they link with neighboring nanosheets to form the rigid platinum structures.

[*] Dr. Y. Song, R. M. Garcia, R. M. Dorin, Dr. H. Wang, Y. Qiu, Prof. J. A. Shelnutt
Advanced Materials Laboratory
Sandia National Laboratories
Albuquerque, NM 87106 (USA)
Fax: (+1) 505-272-7077
E-mail: jasheln@unm.edu
Homepage: http://jasheln.unm.edu/
R. M. Garcia, R. M. Dorin, Dr. H. Wang, Y. Qiu
Departments of Chemistry
Biology and Chemical & Nuclear Engineering
The University of New Mexico
Albuquerque, NM 87106 (USA)
Prof. J. A. Shelnutt
Department of Chemistry
University of Georgia
Athens, Georgia 30602-2556 (USA)

[**] Sandia is multiprogram laboratory operated by Sandia Corporation, a Lockheed Martin Company, for the United States Department of Energy's National Nuclear Security Administration under Contract DEAC04-94AL85000.

Supporting information for this article is available on the WWW under http://www.angewandte.org or from the author.

The network of joined nanosheets replicate the spherical shapes of the templating liposomes (Scheme 1 D; see also Figure 1 a,b) even after the surfactant has been washed away. We have reported on a series of nanoscale Pt dendrites in the form of discrete flat sheets and large convoluted continuous sheets using liposomal aggregates with and without SnOEP as templates.[25,27] For these platinum nanomaterials, a low concentration of SnOEP (or no SnOEP) gives a small number of widely separated seed particles. Depending on the amount of Pt, these conditions result in discrete large circular nanosheets or foam-like materials in which large continuous convoluted dendritic Pt sheets spread over the interfaces of multiple aggregated liposomes.

A reaction system containing aged platinum complex (1 mM), SnOEP (7.9 μM), and 170-nm average-diameter liposomes composed of 1 mM total lipid concentration, when irradiated, gives the hollow Pt nanocages. The average number of SnOEP molecules in a liposome of 160 nm diameter is calculated to be approximately 2400, based on the average cross-sectional areas of 0.39 nm^2 for cholesterol[28] and 0.65 nm^2 for 1,2-dioctadecanoyl-*sn*-glycero-3-phosphocholine (DSPC)[29] and the known concentrations of SnOEP (7.9 μM), DSPC (0.5 mM), and cholesterol (0.5 mM). After irradiation of the reaction mixture with white light for 30 min, a black precipitate forms at the bottom of the reaction vessel leaving a colorless and transparent supernatant, which indicates that the reduction is complete (see Experimental Section and Supporting Information).

Figure 1 a,b shows transmission electron microscope (TEM) images of the nanostructures formed under the above conditions. Hollow nanospheres with diameters in the range from 60 to 200 nm, consistent with the size distribution of the templating liposomes, are observed (see Supporting Information Figure S2). Energy-dispersive X-ray spectroscopy (EDX) confirms that the nanospheres are composed of platinum (Supporting Information Figure S3). The selected-area electron diffraction (SAED) pattern shows that they are polycrystalline (Supporting Information Figure S4). Under these conditions, the coverage of Pt on the liposomes is incomplete, but sufficient to render intact porous spheres (Figure 1 a,b). The yield of the hollow nanospheres is estimated to be 70% based on Pt content in the TEM images. The remaining Pt is in the form of discrete dendritic nanosheets (Figure 1 c) with an average diameter of (12.9 ± 2.3) nm and a thickness of 2 nm as determined previously for the dendritic sheets templated on liposomes.[25] The small Pt dendrites may come partly from liposomes that get relatively small numbers of SnOEP molecules or that receive less light exposure. They may also originate from dendrites that simply fail to link to neighboring dendrites and become dislodged when the surfactant is washed away in preparing the TEM grid. The loose dendrites might also come from broken nanocages, although few large pieces of the nanocages are seen in the TEM images.

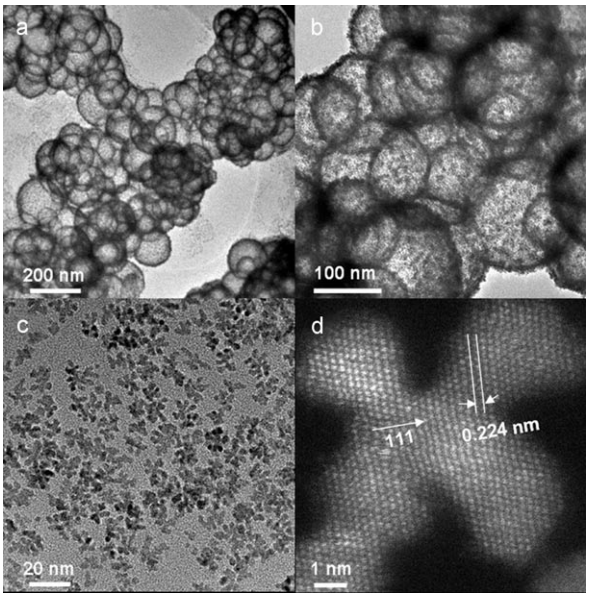

Figure 1. a), b) TEM images of hollow platinum nanocages at different magnifications. c) TEM and d) HAADF scanning TEM image of dendritic nanosheets, which join together upon liposomes to form hollow cages. The [111] direction in the crystal and the spacing of the ⟨111⟩ planes (0.224 nm) is indicated in (d).

Figure 1 d shows a high-angle annular dark-field (HAADF) scanning TEM image of a small Pt dendritic nanosheet. The entire dendrite is one single crystal of platinum as are the others that we have examined. These dendritic nanosheets may grow much larger (> 150 nm) while retaining their single-crystalline nature.[25,27]

Note that the shell thickness appears to be 5 to 10 nm in TEM images (Figure 1 b), while the individual nanosheets are 2 nm thick. The apparent thickness of the shell is mostly due to the tilting of dendrites from their exact edge-on geometry as they curve around the spheres, but some piercing of the outer surface of the bilayer by globular dendrites[25,27] and the low contrast of the images may also contribute to the apparent thickness.

The hollow nanocages agglomerate together to form superstructures, showing some foam-like distortion at the interfaces from the ideal spherical structures. The agglomeration is probably caused by the continuous variation of the solution conditions while the reaction is running, which causes aggregation of liposomes.[30]

Scanning electron microscope (SEM) images of the spherical nanocages are shown in Figure 2 a,b, revealing the hollow interior of several broken cages (Figure 2 a). It appears that some of the interiors of the nanospheres may be interconnected through large openings between adjacent cages (Figure 2 b), providing porosity at a larger scale. The shell thickness of approximately 2 nm, expected from the thickness of the Pt nanosheets,[25,27] is verified by measuring the edges of the broken cages (Supporting Information Figure S5). The high-contrast HAADF scanning TEM[31,32] images confirms the 2-nm thick walls when measured by the width of the bright line formed by the edge of the sphere in Figure 2 c,d. Considering that the outer diameter of the liposomes is up to 200 nm, the ratio of outer diameter and shell thickness is as large as 100:1.

The scanning TEM image of broken cages in Supporting Information Figure S6 more clearly show that the cages are

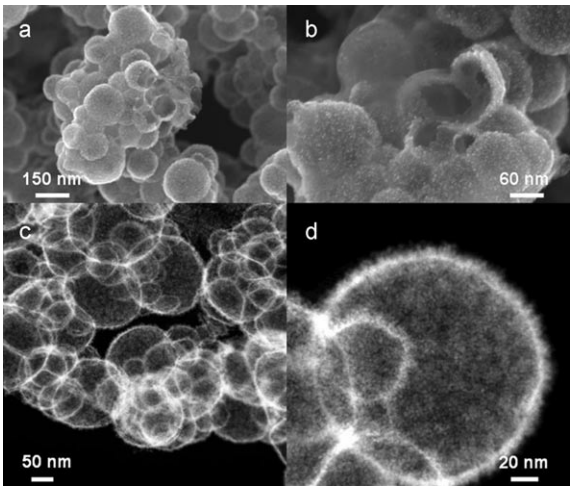

Figure 2. Hollow platinum nanocages: a), b) SEM images at different magnifications; c) and d) HAADF scanning TEM images at different magnifications.

composed of interconnected small dendritic nanosheets. The arms of the nanosheets forming the cages are also barely discernable in Figure 2d. The strong connectivity of dendrites that have grown together in the cages might be expected to provide higher structural stability than for spheres composed of discrete nanoparticles, and indeed the cages do survive under ambient conditions for at least a year, mild sonication, and cleaning by using water, ethanol, and chloroform.

As demonstrated in Figure 3, simply varying the concentration of the Pt complex while holding the SnOEP concentration and light intensity constant controls the structure obtained in the reaction. At low concentrations of Pt complex (0.25 mM), nanoparticles were found in circular groups of the same sizes as the liposomes (Figure 3a), indicating that there was insufficient Pt for growth of even small dendrites. This result is consistent with the suggested formation of Pt seed particles (Scheme 1c). At high concentrations of Pt complex (5 mM), platinum nanocages obtained still have an inner shell thickness of 2 nm, but a furry exterior (Figure 3b) and larger diameter dendritic sheets were observed (Supporting Information Figure S7). Many of the nanosheets show evidence of globular dendrite growth (Supporting Information Figure S7), but most of the dendritic sheets do not show thickening in good agreement with the proposed confined growth within the liposomal bilayers.[25] At the higher concentration of Pt complex (10 mM), the liposomes apparently can not effectively confine the growth of the dendrites and we observe considerable additional globular dendritic growth out from the outer surfaces, especially at interfaces between liposomes (Figure 3c,d).

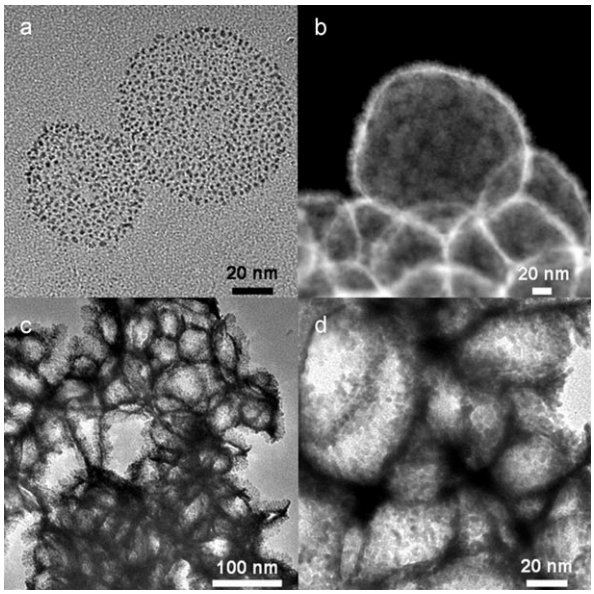

Figure 3. TEM images of platinum nanostructures obtained at various concentration of platinum complex: a) 0.25 mM; b) 5 mM; c) and d) 10 mM. (b) is a dark-field image.

If there is a one-to-one correspondence between a porphyrin molecule and the seed (and thus Pt dendrite) that it produces and, in addition, if the seed particle remains at the location of the porphyrin molecule, then the Pt nanoparticles could be grown and used as nanotags to reveal the location of the Sn-porphyrin in the membrane. The techniques used in this case to produce nanospheres might also be generalized to porphyrin-labeled molecules (e.g., lipids, drug molecules, proteins, or other biological structures) for growing nanometer-sized tags, which can be imaged using electron microscopy to give a high resolution picture of the spatial distribution of the porphyrin-labeled species.

The nanocages offer the opportunity to determine the number of Pt seed particles produced per porphyrin molecule. Since the number of porphyrins per liposome can be calculated, the seed:porphyrin ratio can be determined in two ways—either by counting the number of seed particles in a liposome of known size (e.g., a circle of seeds in Figure 3a) or by determining the average size of the dendrites required for them to link together with others to preserve the spherical structure (estimated by determining the average size from a field of nanosheets as in Figure 1c). Explicitly, the number of porphyrin molecules in the 80-nm diameter liposome of Figure 3a is calculated to be 600, and therefore the 80-nm liposome should ideally contain 600 Pt nanoparticles. Counting the particles using a conservative estimate of the spot density in the image that represents a particle leads to approximately 400 particles; an estimate using a more liberal low-density limit gives about 2000 particles. We find then that the observed number of seeds is within the range of the number of porphyrin molecules in the liposome, and thus the seed:porphyrin ratio obtained by this method is near 1:1 within the large uncertainty in counting introduced by the level of electron density that is deemed to represent a particle.

Another estimate of the seed:porphyrin ratio is given by the average diameter of dendrites required for them to link together to form the nanocages. For the concentrations of lipid and porphyrin used herein, the average liposomal surface area associated with each porphyrin molecule is 33 nm^2. Thus, the average distance between neighboring porphyrin molecules (for idealized hexagonal packing) is

6.2 nm. Therefore, we expect the average diameter of the dendrites to be at least 7 nm for them to join well enough to form a connection. This value is close to the observed average diameter of the dendrites that form the nanocages shown in Figure 1 ((12.3 ± 2.3) nm), again indicating close to one dendrite (or seed) per porphyrin.

The metal nanocages described herein may be suitable for many applications (e.g., as catalysts and electrocatalysts) for which platinum is required to be in an open, low-density, high surface area form. Additional synthetic control over the nanocages can be realized by variation of parameters, such as light exposure, porphyrin concentration, and the size of the templating liposomes. Further, nanocages composed of other metals and alloys can be made.

Experimental Section

SnOEP-containing unilamellar liposomes with a composition of 1:1 DSPC:cholesterol mole ratio were prepared by an extrusion procedure similar to that described previously.[25] In the synthesis, 1 mL of the liposomes ([DSPC] = 0.5 mM, [cholesterol] = 0.5 mM, [AA] = 150 mM, [SnOEP] = 7.9 μM) was mixed with 1 mL of the aged Pt salt solutions (0.5, 2, 10, 20 mM) in a glass vial. The Pt nanocages were produced in the reactions using 2 and 10 mM Pt complex solutions. TEM (200 keV JEOL 2010), HRTEM, HAADF STEM (200 keV JEOL 2010F), EDX, SAED, and SEM (30 keV S-5200) images of the nanostructures were obtained. Additional experimental details are provided in the Supporting Information.

Received: June 15, 2006
Revised: August 18, 2006
Published online: October 25, 2006

Keywords: liposomes · nanostructures · platinum · porphyrinoids · templating

[1] L. R. Hirsch, J. B. Jackson, A. Lee, N. J. Halas, J. West, *Anal. Chem.* **2003**, *75*, 2377 – 2381.
[2] L. R. Hirsch, R. J. Stafford, J. A. Bankson, S. R. Sershen, B. Rivera, R. E. Price, J. D. Hazle, N. J. Halas, J. L. West, *Proc. Natl. Acad. Sci. USA* **2003**, *100*, 13549 – 13554.
[3] S. W. Kim, M. Kim, W. Y. Lee, T. Hyeon, *J. Am. Chem. Soc.* **2002**, *124*, 7642 – 7643.
[4] Y. J. Xiong, B. Wiley, J. Y. Chen, Z. Y. Li, Y. D. Yin, Y. N. Xia, *Angew. Chem.* **2005**, *117*, 8127 – 8131; *Angew. Chem. Int. Ed.* **2005**, *44*, 7913 – 7917; .
[5] P. Jiang, J. F. Bertone, V. L. Colvin, *Science* **2001**, *291*, 453 – 457.
[6] E. Prodan, C. Radloff, N. J. Halas, P. Nordlander, *Science* **2003**, *302*, 419 – 422.
[7] L. H. Lu, R. Capek, A. Kornowski, N. Gaponik, A. Eychmuller, *Angew. Chem.* **2005**, *117*, 6151 – 6155; *Angew. Chem. Int. Ed.* **2005**, *44*, 5997 – 6001; .
[8] M. L. Breen, A. D. Dinsmore, R. H. Pink, S. B. Qadri, B. R. Ratna, *Langmuir* **2001**, *17*, 903 – 907.
[9] Z. J. Liang, A. Susha, F. Caruso, *Chem. Mater.* **2003**, *15*, 3176 – 3183.
[10] Y. Vasquez, A. K. Sra, R. E. Schaak, *J. Am. Chem. Soc.* **2005**, *127*, 12504 – 12505.
[11] Y. G. Sun, Y. N. Xia, *Science* **2002**, *298*, 2176 – 2719.
[12] H. P. Liang, H. M. Zhang, J. S. Hu, Y. G. Guo, L. J. Wan, C. L. Bai, *Angew. Chem.* **2004**, *116*, 1566 – 1569; *Angew. Chem. Int. Ed.* **2004**, *43*, 1540 – 1543; .
[13] J. Y. Chen, B. Wiley, J. McLellan, Y. J. Xiong, Z. Y. Li, Y. N. Xia, *Nano Lett.* **2005**, *5*, 2058 – 2062.
[14] X. Y. Gao, J. S. Zhang, L. Zhang, *Adv. Mater.* **2002**, *14*, 290 – 293.
[15] Y. J. Song, S. R. Challa, C. J. Medforth, Y. Qiu, R. K. Watt, D. Pena, J. E. Miller, F. van Swol, J. A. Shelnutt, *Chem. Commun.* **2004**, 1044 – 1045.
[16] D. B. Zhang, L. M. Qi, J. M. Ma, H. M. Cheng, *Adv. Mater.* **2002**, *14*, 1499 – 1502.
[17] P. R. Selvakannan, M. Sastry, *Chem. Commun.* **2005**, 1684 – 1686.
[18] Y. J. Xiong, J. M. McLellan, J. Y. Chen, Y. D. Yin, Z. Y. Li, Y. N. Xia, *J. Am. Chem. Soc.* **2005**, *127*, 17118 – 17127.
[19] Y. J. Xiong, J. Y. Chen, B. Wiley, Y. N. Xia, *J. Am. Chem. Soc.* **2005**, *127*, 7332 – 7333.
[20] M. S. Wong, J. N. Cha, K. S. Choi, T. J. Deming, G. D. Stucky, *Nano Lett.* **2002**, *2*, 583 – 587.
[21] V. S. Murthy, J. N. Cha, G. D. Stucky, M. S. Wong, *J. Am. Chem. Soc.* **2004**, *126*, 5292 – 5299.
[22] J. N. Cha, H. Birkedal, L. E. Euliss, M. H. Bartl, M. S. Wong, T. J. Deming, G. D. Stucky, *J. Am. Chem. Soc.* **2003**, *125*, 8285 – 8289.
[23] D. R. Rolison, *Science* **2003**, *299*, 1698 – 1701.
[24] E. Antolini, *Mater. Chem. Phys.* **2003**, *78*, 563 – 573.
[25] Y. J. Song, W. A. Steen, D. Pena, Y. B. Jiang, C. J. Medforth, Q. S. Huo, J. L. Pincus, Y. Qiu, D. Y. Sasaki, J. E. Miller, J. A. Shelnutt, *Chem. Mater.* **2006**, *18*, 2335 – 2346.
[26] Y. J. Song, Y. B. Jiang, H. R. Wang, D. A. Pena, Y. Qiu, J. E. Miller, J. A. Shelnutt, *Nanotechnology* **2006**, *17*, 1300 – 1308.
[27] Y. J. Song, Y. Yang, C. J. Medforth, E. Pereira, A. K. Singh, H. F. Xu, Y. B. Jiang, C. J. Brinker, F. van Swol, J. A. Shelnutt, *J. Am. Chem. Soc.* **2004**, *126*, 635 – 645.
[28] R. Villegas, F. V. Barnola, *J. Gen. Physiol.* **1972**, *59*, 33 – 46.
[29] P. Balgavy, M. Dubnickova, N. Kucerka, M. A. Kiselev, S. P. Yaradaikin, D. Uhrikova, *Biochim. Biophys. Acta* **2001**, *1512*, 40 – 52.
[30] J. H. Collier, P. B. Messersmith, *Annu. Rev. Mater. Res.* **2001**, *31*, 237 – 263.
[31] A. V. Crewe, *Chem. Scr.* **1979**, *14*, 17 – 20.
[32] Z. L. Wang, *Adv. Mater.* **2003**, *15*, 1497 – 1514.

